Resveratrol exerts beneficial effects on the growth and metabolism of *Lactuca sativa* L.

Ana Luiza Santos Wagner[1], Fabrizio Araniti[2], Emy Luiza Ishii–Iwamoto[1*] and Maria Rosa Abenavoli[3*]

[1]Laboratory of Biological Oxidations, Department of Biochemistry, State University of Maringa, 87020900 Maringa, Brazil.

[2]Department of Agricultural and Environmental Sciences (DISAA), University of Milan, Via Celoria, 2, 20133 Milan, Italy.

[3]Department of Agriculture, University of Reggio di Calabria, 89124 Reggio Calabria, Italy.

[*]Corresponding author:

Maria Rosa Abenavoli, Phone: +39–0965–196–4350; e–mail: mrabenavoli@unirc.it

Emy Luiza Ishii–Iwamoto, Phone: +55–44–3011–4712; e–mail: eliiwamoto@uem.br

ABSTRACT

In order to assist sustainable agriculture, new strategies and methods are being used based on the utilization of new natural molecules. These natural compounds can be used as potential natural crop protectors and growth promoters, and the elucidation of their modes/mechanisms of action can represent a big step towards cleaner agriculture free of agrochemicals. In the present paper, the mechanisms underlying the effects of exogenous resveratrol (R), a natural phytoalexin found in plants, on *Lactuca sativa* metabolism were investigated through physiological and metabolomic approaches. The results highlighted that R stimulates the growth of lettuce. A reduction of the $O_2^{\cdot -}$ production in R–treated seedlings and an increase in the photosynthesis efficiency was observed, indicated by a higher *F*v/*F*m. The metabolomic analysis of lettuce seedlings treated with R identified 116 metabolites related to galactose, amino acids, sugar and nucleotide sugar, and ascorbate and aldarate metabolisms. Increased content of some polyamines and several metabolites was also observed, which may have contributed to scavenging free radicals and activating antioxidant enzymes, thus reducing oxidative damage and improving PSII protection in R–treated seedlings.

Keywords: crop protector, growth promoter, metabolomic analyses, photosynthesis, plant development.

1. INTRODUCTION

Resveratrol (3,5,4′–trihydroxystilbene) is a phenolic micronutrient naturally found in a few plant species, including grapes, berries, peanuts, and pines (Shishodia and Aggarwal 2006; Harikumar and Aggarwal 2008). Over the last 50 years, the resveratrol research has increased due to its promising human health benefits such as the antioxidant, anticarcinogenic, antibacterial, anti-inflammatory, cardio– and neuroprotective properties (Belchí–Navarro et al. 2012; Shi et al. 2014; Salehi et al. 2018; Vestergaard and Ingmer et al. 2019). The mechanism underlying these beneficial effects is its ability to activate sirtuin-like protein deacetylases, redox–sensing enzymes involved in modulating metabolism regulation, stress responses, ageing processes, and longevity (Halls and Yu 2008; Gertz et al. 2012).

In plants, resveratrol plays a crucial role in plant response to biotic and abiotic stresses (Liu et al. 2019), such as UV radiation and pathogens attacks (Elshaer et al. 2018; Vestergaard and Ingmer 2019), boron toxicity (Sarafi et al. 2017), ozone

(Grimmig et al. 2002), and saline stress (Kostopoulou et al. 2014). In particular, under stress conditions, plants trigger a complex biochemical system to increase the resveratrol synthesis and accumulation to confer protection (Hammerschmidt 1999; Bednarek and Osbourn 2009; Ahuja et al. 2012; Elshaer et al. 2018; Vestergaard and Ingmer 2019). Some authors suggested that this protection was due to its ability to scavenge diverse reactive oxygen species (ROS), increasing the cellular defence system (Truong et al. 2018). King et al. (2006) demonstrated that resveratrol reduced damage to cell membranes, maintaining their stability and limiting ROS stress in transgenic plants. Moreover, in tomato plants, the resveratrol accumulation caused an increase in ascorbic acid, glutathione, and antioxidant enzymes, which limited damages caused by ROS (D'Introno et al. 2009).

The beneficial resveratrol effects as a potential natural crop protector were also achieved by its exogenous application (Pociecha et al. 2014; Sarafi et al. 2017). In particular, Pociecha et al. (2014) observed that the resveratrol applied on powdery mildew infected–wheat leaves increased the phenolics metabolism and photosynthetic efficiency, reducing the damage during pathogenesis. Furthermore, before UV- C treatment, the resveratrol application to peanut plants mitigated the damage symptoms of rusty spots and leaf wilt (Tang et al. 2010) and delayed the decay process during apple fruit storage (Gónzalez–Urena et al. 2003).

For all these reasons, researchers are focused on transgenic plants production in which the resveratrol synthase gene was overexpressed (Delaunois et al. 2009). The *sts* overexpression in tobacco, rice, apple, and grape increased resveratrol content conferring higher resistance to abiotic and biotic stresses (Dai et al. 2015; Zheng et al. 2015; Chu et al. 2017). For example, in transgenic rice seedlings, the resveratrol content was significantly increased (5–8 fold) under UV–C exposure compared to those grown under normal conditions (Zheng et al. 2015).

Although most studies had mainly focused on the potential antimicrobial, antibacterial (Mattio et al. 2020), and antioxidant activity in response to abiotic and biotic stresses (Hasan and Bae 2017), few investigations have been carried out on the resveratrol effect on plant metabolism, regardless its role in the induction of the protective mechanisms (Bruno and Sparapano 2006; Liu et al. 2019).

Recently, Mantovanelli et al. (2020) studied the effect of exogenous resveratrol on seed germination, seedling growth, and mitochondrial energy metabolism in the crop/weed system, *Zea mays*/*Ipomoea grandifolia*. They demonstrated that resveratrol

stimulates maize seedling growth, inhibiting, at the same concentration, the weed *I. grandifolia*. Under the same condition, the authors found a decrease in the respiratory activity due to the cytochrome–oxidase pathway in *I. grandifolia*, but not in *Z. mays* roots. These data suggest that the exogenous resveratrol can modify the metabolism of different plants, even in non–stressful conditions, a question that so far has not been examined in detail. In this respect, the present study aimed to deeper insight into the mechanisms underlying the action of exogenous resveratrol on plant metabolism through physiological and metabolomic approaches. We used *Lactuca sativa*, a sensitive crop species to natural and synthetic compounds (Araniti et al. 2012).

2. Materials and methods

2.1 Dose-response curves

Lactuca sativa L. (var. Parris Island COS) seeds were sterilized with 2.0% sodium hypochlorite solution for 10 min and washed in distilled water. Then, 15 sterilized seeds were sown in Petri dishes (100 x 100 mm) containing a double layer of filter paper, moistened with 6 ml of sterile deionized water (control) and an aqueous solution of resveratrol (6.25, 12.5, 25, 50, 100, 200, and 400 µM) and transferred into a ventilated climatic chamber with 16/8 h (light/dark) photoperiod, 25±1 ºC temperature, 120 µmol m^{-2} s^{-1} light intensity provided by a cold white fluorescent lamp (Polylux XL FT8, 55 W 8440), and 55% relative humidity for 6 d.

After 6 d of treatment, the germinated seeds, which emitted at least 2 mm of radicle in addition to the integument, were counted, and the total germination was determined as described by Chiapusio et al. (1997). Then, root length was measured, roots and aerial parts were collected, and their fresh weight was evaluated separately. Plant material was then oven-dried for one week at 60 ºC in order to determine the dry weight. The average of aerial part fresh weight in response to each resveratrol concentration allowed us to determine the hormetic concentration (stimulating dose) through a non–linear regression model using a log-logistic function proposed by Beltz et al. (2005). This equation is widely used for evaluating the biphasic effects [stimulatory (hormesis) and phytotoxic (ED_{50})] of natural and synthetic products (Table Curve 2d by Systat Software). The identified stimulatory concentration was then used for all the physiological and metabolic experiments.

2.2 Leaf osmotic potential [Ψ(π)]

After 6 d of treatment, leaf Ψ(π) was measured on four treated (100 µM resveratrol) and non–treated (0 µM) leaves according to Araniti et al. (2016). Treated and non–treated leaves were collected and frozen at –20 ºC. After 24 h, leaves were squeezed into a syringe (the first drop was thrown away to avoid broken cell fluid contamination), the extract was collected, and the leaf Ψ(π) was measured with a cryoscopic osmometer (Osmomat 030, Gonatec). The leaf Ψ(π) was expressed in megapascal (MPA).

2.3 In situ semi-quantitative determination of H_2O_2 and $O_2^{\cdot-}$

Hydrogen peroxide was determined based on Araniti et al. (2016) with some modifications. After resveratrol treatment for 6 d, four fully expanded treated (100 µM) and non–treated (0 µM) leaves were cut, vacuum infiltrated for 5 min in 3,3'–diaminobenzidine (DAB) (1 mg ml^{-1}) solution (pH 3.8), and incubated for 8 h in the same solution in the dark. After the incubation period, leaves were illuminated for 1 h and rinsed twice in pure ethanol to remove the pigments. Bleached leaves were stored in 80% glycerol.

For $O_2^{\cdot-}$ determination, four fully expanded treated (100 µM resveratrol) and non–treated (0 µM) leaves were vacuum infiltrated for 5 min with a 0.65 mg ml^{-1} solution of sodium azide (NaN_3) in potassium phosphate buffer (pH 7.8) containing 0.1% of nitroblue tetrazolium (NBT) (Halliwell and Gutteridge 1985), and incubated in darkness for 20 min in the same solution. After the incubation, leaves were illuminated until the appearance of stains. Image analysis was used to quantify H_2O_2 and $O_2^{\cdot-}$, stained areas using the software Image ProPlus v.6.0 (Media Cybernetics Inc., Bethesda, MD, USA).

2.4 Chlorophyll a fluorescence parameters

The chlorophyll *a* fluorescence in treated (100 µM resveratrol) and non–treated (0 µM) lettuce seedlings was monitored at the end of the treatment (6 d), using the Maxi–Imaging–PAM Chlorophyll Fluorescence System fluorometer (Walz, Effeltrich, Germany), as previously described by Araniti et al. (2017). The maximum efficiency of photosystem II (PSII) in dark-adapted state (*F*v/*F*m), the apparent electron transport rate (ETR), the effective PSII photochemical quantum yield (ϕ_{II}), the quantum yield of regulated emission of energy in the form of heat (ϕ_{NPQ}), and the non–regulated emission

of energy in the form of fluorescence (ϕ_{NO}) were evaluated. The photosynthetic response was monitored for 5 min, and fifteen measurements were obtained for each parameter at each measuring time.

2.5 Stomatal density and size

Immediately after leaf detaching, both stomatal density (number of stomata per unit leaf area) and size (length between the junctions of the guard cells at each end of the stomata and width between the distal side of the guard cells) were evaluated on non–treated (0 µM) and treated plants (100 µM resveratrol), using an epifluorescence microscope system (Olympus bx53) used in bright field and expressed as a percentage compared to the control (Malone et al. 1993; Xu and Zhou 2008). It should be specified that stomatal length might indicate the maximum potential opening of the stomatal pore, but not the aperture that actually occurs.

2.6 Untargeted metabolomic analysis

2.6.1 Samples extraction, derivatization, and analytical conditions

To evaluate the impact of resveratrol on plant metabolism, non–treated (0 µM) and treated (100 µM) leaves were collected after 6 d, and the metabolome was extracted and derivatized as previously described by Lisec et al. (2006).

One µl of the derivatized extract was injected into a GC–MS apparatus (Thermo Scientific) equipped with a MEGA S.r.l. 5MS capillary column (30 m × 0.25 mm × 0.25 µm) with 10 m of pre-column. Injector and source were settled at 250 °C and 260 °C temperatures, respectively. Samples were injected in splitless mode with helium as a carrier gas with 1 ml/min flow. They were then analyzed using the programmed temperature proposed by Landi et al. (2020): isothermal 5 min at 70 °C, followed by a 5 °C/min ramp to 350 °C, and a final 5 min heating at 330 °C. Mass spectra were recorded in electronic impact (EI) mode at 70 eV, scanning at 40–600 m/z range and scanning time 0.2 s. The mass spectrometric solvent delay was settled as 7 min. *n*–Alkane standards (C10–C40 all even) and blank solvents were injected at scheduled intervals for instrumental performance, tentative identification, and monitoring shifts in retention indices.

2.6.2 Analyses of GC–MS Metabolomics Data

Raw GC–MS data were analyzed using the software MS–DIAL ver. 4.48 coupled with a home built EI spectra libraries based on GOLM database, MassBank; Mass Bank of North America, etc. (Kopka et al. 2005; Tanaka et al. 2010; Tsugawa et al. 2015).

MS–DIAL analysis was settled as previously reported by Landi et al. (2020). Metabolite annotation was carried out comparing the retention index and the spectra similarity of the samples with those of the libraries, following the Metabolomics Standards Initiative (MSI) of the International Metabolomics Society. In particular, reported annotations were considered at level 2 (putative annotation based on spectral library similarity) or level 3 (putatively characterized compound class based on spectral similarity to known compounds of a chemical class) as suggested by Sumner et al. (2007).

2.7 Experimental design and statistical analysis

All the experiments were carried out in a completely randomized design with n = 3 for dose–response curves, n = 5 for leaf osmotic potential, and n = 4 for chlorophyll *a* fluorescence parameters, leaf stomatal density, width and length, and metabolomic analysis. For chlorophyll *a* experiments data were analyzed through the Grubbs test (XLSTAT Addinsoft version 2014.05.03) to evaluate the presence of outliers, which were successively excluded from the mean average.

Dose-response curves and physiological data were expressed as mean ± standard errors (SE) and were analyzed using analysis of variance (ANOVA) with Tukey's Honestly Significant Difference (HSD) or Student's *t*-test as post–hoc ($p \leq 0.05$). The stimulation parameter was calculated, tightening the dose-response curve's raw data through a non–linear regression log-logistic equation model proposed by Beltz et al. (2005).

Metabolomic experiments were carried out using a completely randomized design with six replications for each treatment (n = 6), and data were zanalyzed using the software Metaboanalyst 5.0 (Chong and Xia 2020). Data normalization was carried out using the internal standard (0.02 mg ml^{-1} Ribitol) based normalization functions in the MS–DIAL software. The internal standard normalized dataset was transformed through "Log2 normalization" and Pareto scaled. The data were then classified through unsupervised multivariate Principal Component Analysis (PCA). The output comprised score plots to visualize the contrast between different samples and loading plots to

explain the cluster separation. Metabolite variations were presented as a heatmap reporting only significant features of the t–test analysis (see below). Partial Least–Squares discriminant analysis (PLS-DA) was used to highlight differences between the two treatments (0 and 100 µM resveratrol).

Data were then analyzed through the univariate *t*-test ($p \leq 0.05$) to highlight statistical differences among single metabolites and treatment. A False Discovery Rate (FDR) was applied to the nominal *p*–values to control false-positive findings.

Finally, to identify the metabolites coverage and the main altered pathways under resveratrol treatment, data were analyzed using the Metaboanalyst enrichment analysis and pathway analysis tools.

3. RESULTS

3.1 Germination and seedlings growth bioassays

Resveratrol did not affect lettuce seed germination at all the concentrations applied. Conversely, resveratrol treatment caused a strong stimulatory effect on *L. sativa* growth, especially on the aerial part, where, at all concentrations (6.25–400 µM), it significantly increased fresh weight compared to the control (Figure 1D). The raw data obtained from the aerial part fresh weight allowed us to estimate the stimulatory dose, which was equal to 100 µM (Fig. 1D). This concentration was used in all the subsequent experiments. The highest resveratrol doses (100–400 µM) also significantly increased the aerial part dry weight (Figure 1F).

Resveratrol treatment also increased the root fresh weight at 25 and 200 µM (Figure 1C), while both root length (Figure 1B) and dry weight (Figure 1E) were not affected by resveratrol.

3.2 In situ semi-quantitative determination of $O_2^{\cdot -}$ and H_2O_2

As shown in Figure 2, leaves of control (Figure 2A) and resveratrol–treated (Figure 2B) seedlings showed the same colour and intensity, indicating that this potential elicitor did not alter the production of H_2O_2 in *L. sativa* leaves.

By contrast, resveratrol markedly reduced the superoxide production in *L. sativa* leaves. Indeed, treated leaves showed fewer and weaker colour regions (Figure 3B) than the control (Figure 3A), supporting a reduction in the $O_2^{\cdot -}$ production under resveratrol treatment.

3.3 Leaf stomatal density, size and width, and leaf osmotic potential [Ψ(π)]

Stomata were open with turgid guard cells in both non–treated and treated plants (Figure 4A, B). Resveratrol treatment did not alter stomatal density and length (Figure 4C, E) but increased stomatal width (Figure 4D).

Concerning leaf Ψ(π), the data pointed out that resveratrol (100 µM) did not alter leaf osmotic potential of *L. sativa* compared to the control (Figure 5).

3.4 Chlorophyll a fluorescence parameters

Resveratrol treatments significantly stimulated the PSII system. In particular, the maximum quantum efficiency of dark–adapted PSII (*F*v/*F*m), the effective PSII photochemical quantum yield (ϕ_{II}), the quantum yield of regulated energy emission in the form of heat (ϕ_{NPQ}) were weakly but significantly stimulated by resveratrol treatment (Figure 6A-D). On the contrary, the non–regulated energy emission in the form of fluorescence (ϕ_{NO}) was significantly reduced by the treatment (Figure 6E). No differences in ETR parameter were observed (Fig. 6B).

3.5 Untargeted metabolomic analysis

The GC–MS–driven untargeted metabolomic analysis of resveratrol–treated seedlings allowed us to annotate and quantify 116 metabolites and extract 1005 unknown EI–MS shared features (Supplementary Table S1 file excel).

Both annotated and unknown metabolites (Supplementary Table S1 file excel), processed through MS–DIAL, were reported as supplementary data displaying their retention times, quantmass, signal/noise ratio (S/N), RI similarity, total similarity, total spectrum similarity, and relative abundances.

A KEGG–based enrichment analysis (a method to identify classes of metabolites that are over-represented in a large set of metabolites and might have an association with treated seedlings phenotype) of the metabolic pathway revealed enrichment of galactose metabolism, amino sugar and nucleotide sugar metabolism, ascorbate and aldarate metabolism, among others (Figure 7A and Supplementary Table S1 file excel). Most of these annotated metabolites belonged to the primary metabolism (amino acids, sugars, organic acids, etc.) and in minor part to plant specialized metabolites (e.g., 2,3–dihydroxybenzoate, quinic acid, etc.).

The pathway analysis, which combines enrichment and topology analysis, pointed out that 28 pathways were significantly changed between the two treatments

(Figure 7B and Supplementary Table S1 file excel). Still, only 8 were characterized by an impact higher than 0.2: starch and sucrose metabolism; alanine, aspartate and glutamate metabolism; glycine, serine and threonine metabolism; arginine biosynthesis; galactose metabolism; ß–alanine metabolism; glyoxylate and dicarboxylate metabolism; pantothenate and CoA biosynthesis (Figure 7B and Supplementary Table S1 file excel).

The *t*–test analysis pointed out that 68 out of 116 metabolites were differentially produced between treatments. These metabolites mainly belonged to chemical classes of the amino acids (aspartic acid, glutamic acid, alanine, serine, among others), organic acids (tartaric acid, succinic acid, glyceric acid, among others), sugars and sugar alcohols (fructose, cellobiose, arabinose, galactinol, xylitol, among others), polyamines (putrescine and ornithine), etc. (Table 1).

Except for eleven metabolites (putrescine, DL–ß–hydroxybutyric acid, L–rhamnose, succinic acid, glyceric acid, glycerol–3–galactoside, creatinine, uridine, threonic acid, mannose, and methylmalonic acid), all the statistically significant metabolites were stimulated by resveratrol treatment (Table 1).

The unsupervised Principal Component Analysis (PCA) was carried out on blank samples and all three samples group to demonstrate the system suitability. The PCA Score Plot, built on the first (PC1) and the second component (PC2), revealed clear discrimination of sample groups against blanks, highlighting model robustness (Supplementary Figure S1A). The components separated control and treated groups with no outliers (Supplementary Figure S1), indicating that the metabolomic analysis was reliable and could reflect the metabolic profile changes induced by the resveratrol treatment.

Both unsupervised PCA runs on MS-DIAL suggested that metabolites (Supplementary Figure S1B) and unknown features (Supplementary Figure S1C) were useful for clear sample groups' discrimination. Further, both unsupervised PCA analyses (Figure 8A) and Supervised Partial Least Squares Discriminant Analysis (PLS-DA), carried out only on the annotated metabolites (Figure 8B), demonstrated group separation with the first 2 principal components (PCs), explaining 72.2% variance for PCA and 71.5% variance in PLS-DA score plots. The permutation test validated the PLS-DA model's robustness, highlighting a high R^2 and Q^2 for both latent variables (Supplementary Figure S2).

PLS–DA derived variable importance of projection (VIP) scores (built on the first 30 metabolites with a VIP score higher than 1.4) revealed DL–ß–hydroxybutyric

acid, palatinitol, gentiobiose, L–ornithine, L–glutamic acid, among others, like the ones with the highest VIP scores between the two treatments (Figure 8C).

Finally, the cluster analysis on the top of the heat map (reporting in a false scale colour the variation of significantly different metabolite concentrations for each sample and replicate) further confirmed total discrimination between the two treatments, which clustered separately (Figure 8D).

4. Discussion

Resveratrol did not significantly affect the lettuce seed germination, reproducing the observation of Mantovanelli et al. (2020) in *Z. mays* and *I. grandifolia*. Similar results were also reported in radish seeds where resveratrol did not have intensive germination–stimulating properties, unlike protectors to ethanol seed sterilization treatment (Balanov et al. 2021). Conversely, it significantly stimulated fresh and dry weight of the aerial part of lettuce, already at low concentrations, leaving unchanged the length and weight of the root system. This positive effect was already observed in maize seedlings, although only at 440 µM resveratrol concentration (Mantovanelli et al. 2020). In particular, a dose-dependent increase in fresh weight, ranging from 6.25–400 µM, was observed. By contrast, the positive effect on dry weight was observed at 100–400 µM range. The primary root length of lettuce was not affected by resveratrol, although a significant increase in root fresh weight was observed at 200 µM resveratrol, confirming the trend already reported in maize (Mantovanelli et al. 2020). However, Mantovanelli et al. (2020) demonstrated that at concentrations above 440 µM, the effects on *Z. mays* seedling growth shift from stimulation to inhibition, an action that has correlated to interference of resveratrol on energy metabolism of maize root mitochondria.

Thereby, our results indicated that the aerial part could be considered a main target of resveratrol. Thus, we focused on a better understanding of the resveratrol activity using the hormetic value calculated using the equation (also used for ED_{50} calculation) proposed by Belz et al. (2005). One hundred µM resveratrol confirmed the beneficial effect of this elicitor on lettuce aerial part (stem and leaves) and its ability to stimulate plant growth when exogenously applied (Pociecha et al. 2014; Mantovanelli et al. 2020). Mantovanelli et al. (2020) hypothesized that resveratrol is structurally similar to the synthetic oestrogen diethylstilbestrol, naturally produced by plants, which stimulated plant growth, cell division, and pollen germination (Janeczko and Skoczowski 2005). They further suggested a behaviour similar to brassinosteroids,

which induced plants tolerance under stress conditions by increasing the antioxidant activity (Fariduddin et al. 2013) and stimulated plant growth (Clouse and Sasse 1998). Thus, we hypothesized that the stimulatory effect of resveratrol on lettuce could be linked to its potent ROS scavenger ability (Stojanović et al. 2001). In plants, ROS, generated in several organelles (Dietz et al. 2016; Huang et al. 2016), included hydroxyl radicals ($^{\bullet}OH$) and superoxide anions ($O_2^{\cdot-}$), and molecular states, hydrogen peroxide (H_2O_2) and singlet oxygen ($^1O_2$) (Apel and Hirt 2004; Mittler et al. 2004). While ROS are important for plant growth, performing many physiological processes (Elstner 1987; Choudhury et al. 2017), their overproduction, under various biotic and abiotic conditions, causes lipid peroxidation, DNA and protein damage, resulting in perturbation of the cellular redox state that can ultimately lead to oxidative stress and cell death (Gill and Tuteja 2010; Dumont and Rivoal 2019). Interestingly, 100 µM resveratrol reduced the $O^{\cdot-2}$ production, leaving unchanged the H_2O_2 content. In particular, the superoxide anion, produced in chloroplasts, mitochondria, endoplasmic reticulum, and peroxisomes under their normal metabolism (Sharma et al. 2012), is an unstable molecule (Juan et al. 2021) rapidly converted to hydrogen peroxide, permeable to the membrane. Transmembrane NADPH–oxidases (NOXs) and the mitochondrial and chloroplastic electron transport chain (ETC) are the most important enzymes and organelles producing $O^{\cdot-2}$ and H_2O_2 (Fisher 2009). However, it is not clear whether resveratrol acts directly as anti-ROS, or indirectly by blocking ROS production by enzymes such as NADPH oxidase (NOX) or by influencing the expression of cellular pro– and antioxidants. The downregulation of NOXs after resveratrol treatment to protect mammalian cells from oxidative functional damages is strongly demonstrated (Block and Gorin 2012).

The importance of the antioxidant network in maintaining high rates of photosynthesis has been demonstrated in many studies (Foyer and Shigeoka 2011) since ROS overproduction and accumulation can also inhibit photosynthesis, limiting plant growth and yield (Mittler and Blumwald 2010). Thus, resveratrol's maintenance of $O_2^{\cdot-}$ low concentration could induce a higher photosynthetic efficiency. For example, by preserving ROS homeostasis, melatonin also helps to maintain a better performance of the photosynthetic process under salinity stress (Li et al. 2019). Furthermore, Pociecha et al. (2014) demonstrated that resveratrol stimulated photosynthetic efficiency during pathogenesis, influencing the energy flux parameter for electron transport and improving the stability and efficiency of membranes. Among Chlorophyll fluorescence

(ChlF) parameters, the quantum efficiency of photosystem II (PSII) in the dark- and light-adapted conditions (*F*v/*F*m and *F*v'/*F*m') are usually good indicators of photosynthetic activity, physiological function, as well as healthy and stress conditions (Jia et al. 2019). In particular, *F*v/*F*m, which indicates the initial maximal efficiency of photons captured by open PSII reaction centres, is used as an indicator of health and plant growth (Feng et al. 2015) more than *F*v'/*F*m' (Jia et al. 2019). For example, under a range of nitrogen (N) fertilizer, the *F*v/*F*m increased along with N application (Liu et al. 2008). By contrast, a reduced value of *F*v/*F*m was indicative of the probable physical damage at the level of the antenna complex accompanied by a reduction in the PSII efficiency as observed under stress conditions such as drought (Maxwell and Johnson 2000; Prieto et al. 2009).

Interestingly, the results indicated that all the chlorophyll fluorescence parameters were significantly and positively affected by the treatment. In particular, the increase in *F*v/*F*m ratio, higher in the resveratrol–treated leaves, suggest a higher stability rate of the complex PSII/LHC and increasing lettuce growth. This increase suggests a higher efficiency of the antenna complexes that, driving the excitation energy to the electron transport chain, increase the efficiency of the light-adapted PSII (significantly stimulated by resveratrol treatment). In addition, in optimal conditions, plants treated with resveratrol pointed out a higher ability to dissipate the energy in excess in the form of heat and a lower loss of energy in the non-regulated form of fluorescence. All these data suggest that resveratrol acted in lettuce seedlings as a PSII enhancer. Similar effects were previously observed on Arabidopsis and maize seedlings treated with low doses of the natural compounds protocatechualdehyde and *trans*-cinnamic acid, respectively (Araniti et al. 2018; Martínez-Peñalver et al. 2012).

The resveratrol action on photosynthesis may also be associated with the stimulation of ornithine, a polyamine that scavenges free radicals and activates some antioxidant enzyme activities, subsequently reducing oxidative damage (Hussein et al. 2019; Liu et al. 2015), and are essential in the regulation of plant growth and development (Martin–Tanguy 2001). In lettuce treated seedlings, a high level of L–ornithine, the precursor of polyamines, was reported, whereas the treatment significantly reduced putrescine. Although no proof is available concerning the role of exogenous resveratrol on polyamine biosynthesis, several studies on mammalian cells highlighted that resveratrol negatively affects the enzyme ornithine decarboxylase (Kanduja et al. 2004; Wolter et al. 2003). The ornithine decarboxylase is involved in the

conversion of ornithine to putrescine. In addition, previous studies demonstrated that although putrescine acts as an osmoprotectant in plants, its overproduction negatively impacts the oxidative state of the cells because of its enhanced turnover (Mohapatra et al. 2009).

Therefore, the ornithine accumulation and the consequent reduction in putrescine production could be due to the resveratrol-induced inhibition of the ornithine decarboxylase activity; at the moment, it is just speculation that should be explored in depth.

All these findings again support thatresveratrol could exert a protective effect on PSII, allowing us to consider it as a PSII enhancer.

On the other hand, resveratrol treatment did not affect stomatal density and size but induced a higher stomatal width, suggesting a potential increased gas exchange in treated plants. This phenomenon, also supported by the increase of PSII efficiency, is commonly observed with natural compounds belonging to the classes of phenols. For example, An et al. (2016) demonstrated that the accumulation of flavonols in the guard cells, induced by an elicitor, is involved in ROS detoxification and the ABA–induced inhibition of stomatal closure. The stomatal width is an important indicator of the stomatal aperture being related to a higher rate of CO_2 exchange and photosynthetic efficiency. Therefore, the results suggest that resveratrol, acts as a PSII protector and/or stimulating agent, bursting the metabolism, as also suggested by the metabolomic analysis.

Among the metabolic pathways, resveratrol significantly enriched the galactose metabolism and the ascorbate and aldarate metabolism (the first and third most enriched pathway). Both pathways are closely related since the galactose pathway is involved in ascorbate biosynthesis (Smirnoff and Wheeler 2000). Interestingly, besides the high accumulation of galactose observed in resveratrol–treated plants, an accumulation of dehydroascorbic acid (DHA) was also found. It should not be excluded that the increase in DHA content could be due to the oxidation of ascorbic acid (AA) during sample handling and analysis, meaning that treated plants were particularly rich in ascorbate content. In fact, it has been reported that AA is unstable in aqueous solutions under aerobic conditions (extraction and derivatization conditions) being converted in DHA (Levandoski et al. 1964; Dewhirst and Fry 2018).

Among different pathways for ascorbate biosynthesis (Jain and Nessler 2000; Agius et al. 2003; Lorence et al. 2004), galactose is one of the most important pathways

recently discovered. It is well known that high AA content was positively correlated with high galactose level induced by higher activity of L–galactose–1–phosphate phosphatase (GPP) in rice (Zhang et al. 2015), or L–galactose guanyltransferase in *Arabidopsis* (Laing et al. 2007; Bulley et al. 2009), or L–galactose DH in tomato cultivars (Cervilla et al. 2007), or GPP and GDP–D–mannose–3′,5′–epimerase (GME) co-expression in *Nicotiana benthamiana* (Laing et al. 2015).

The alterations in galactose and starch and sucrose metabolisms were generally underlined by a high accumulation of different classes of sugars, including polyols, which play a pivotal role in providing carbon and energy for the normal functioning of cellular metabolism and in regulating the growth and development of plants acting as signal molecules. The osmoprotectant roles of sugars (glucose, fructose, trehalose, etc.) and sugar alcohols (glycerol, inositol, maltitol, etc.), all stimulated by resveratrol treatment, have been widely accepted. They could regulate the osmotic adjustment and/or provide membrane protection and ROS scavenging activity under stress (Kerepesi and Galiba 2000; Murakeözy et al. 2003; Ahmad et al. 2008; Livingston et al. 2009; Van den Ende and Valluru 2009; Koyro et al. 2012). Among them, trehalose should be mentioned in response to resveratrol treatment. This molecule plays an important role either in optimal or under stress conditions, acting as an osmoprotectant or osmolyte protecting membranes and proteins and decreasing aggregation of denatured proteins (Ashraf and Harris 2004; Koyro et al. 2012).

Furthermore, besides sugar accumulation, resveratrol–treated lettuce seedlings were characterized by an accumulation of several proteinogenic amino acids (glutamic acid, aspartic acid, alanine, among others), known to be involved either in osmoprotection or in protein biosynthesis and biomass production (Rai 2002).

5. Conclusion

Our results revealed that the stimulation observed in *L. sativa* growth by resveratrol treatment was due to a stimulus in the cellular metabolism and a decrease of oxidative damage. The photosynthesis efficiency was enhanced, as we observed a reduction in the $O_2^{\cdot -}$ concentration and an increase in several PSII efficiency parameters (Fv/Fm, ϕ_{II} and ϕ_{NPQ}), indicating greater stability of the PSII/LHC complex. The metabolomic analysis showed, in resveratrol–treated seedlings, a higher concentration of ornithine and several metabolites with osmoprotectants activity,which can be related to decreased oxidative damage by scavenging free radicals and activating antioxidant

enzymes. Therefore, the joint regulation of biochemical pathways involved in energy and amino acid metabolism, associated with the regulation of cellular superoxide levels, might be the main reason for the protective and enhancing activity observed on PSII efficiency, promoting plant growth.

Acknowledgements

This work was supported by grants from the Araucária Foundation (112/2010) do Estado do Paraná, National Council for Scientific and Technological Development (CNPq). Ana Luiza Santos Wagner fellowship holder from the Coordination for the Improvement of Higher Education Personnel (CAPES).

Conflict of interest

The authors declare that they have no conflict of interest.

References

Agius F, González–Lamothe R, Caballero JL, Muñoz–Blanco J, Botella MA, Valpuesta V. 2003. Engineering increased vitamin C levels in plants by overexpression of a D–galacturonic acid reductase. Nat Biotechnol. 21(2):177–181.

Ahmad P, Sarwat M, Sharma S. 2008. Reactive oxygen species, antioxidants and signaling in plants. J Plant Biol. 51:167–173.

Ahuja I, Kissen R, Bones AM. 2012. Phytoalexins in defense against pathogens. Trends Plant Sci. 17(2):73–90.

An Y, Feng X, Liu L, Xiong L, Wang L. 2016. ALA–induced flavonols accumulation in guard cells is involved in scavenging H_2O_2 and inhibiting stomatal closure in *Arabidopsis* cotyledons. Front Plant Sci. 7:1713.

Apel K, Hirt H. 2004. Reactive oxygen species: metabolism, oxidative stress, and signal transduction. Annu Rev Plant Biol. 55:373–399.

Araniti F, Graña E, Krasuska U, Bogatek R, Reigosa MJ, Abenavoli MR, Sánchez–Moreiras AM. 2016. Loss of gravitropism in farnesene–treated *Arabidopsis* is due to microtubule malformations related to hormonal and ROS unbalance. PLoS ONE. 11(8):e0160202.

Araniti F, Lupini A, Mauceri A, Zumbo A, Sunseri F, Abenavoli MR. 2018. The allelochemical *trans*-cinnamic acid stimulates salicylic acid production and galactose

pathway in maize leaves: A potential mechanism of stress tolerance. Plant Physiol. Biochem. 128: 32-40.

Araniti F, Lupini A, Sunseri F, Abenavoli MR. 2017. Allelopatic potential of *Dittrichia viscosa* (*L.*) W. Greuter mediated by VOCs: a physiological and metabolomic approach. PLoS ONE. 12(1):e0170161.

Araniti, F., Sorgonà, A., Lupini, A., & Abenavoli, M. R. 2012. Screening of Mediterranean wild plant species for allelopathic activity and their use as bio-herbicides. Allelopathy Journal, 29(1): 107-124.

Ashraf M, Harris PJC. 2004. Potential biochemical indicators of salinity tolerance in plants. Plant Sci. 166(1): 3–16.

Balanov PE, Smotraeva V, Abdullaeva MS, Fedorov AV, Ivanchenko OB, Volkov MP. 2021. Protective properties of resveratrol in biological systems containing ethanol. Conf Ser Earth Environ Sci. 640:052029.

Bednarek P, Osbourn A. 2009. Plant–Microbe interactions: chemical diversity in plant defense. Science. 324(5928):746–748.

Belchí–Navarro S, Almagro L, Lijavetzky D, Bru R, Pedreño MA. 2012. Enhanced extracellular production of trans–resveratrol in *Vitis vinifera* suspension cultured cells by using cyclodextrins and methyljasmonate. Plant Cell Reports. 31(1):81–89.

Belz RG, Hurle K, Duke SO. 2005. Dose–response—a challenge for allelopathy? Nonlinearity Biol Toxicol Med. 3(2):nonlin–003.

Block K, Gorin Y. 2012. Aiding and abetting roles of NOX oxidases in cellular transformation. Nat Rev Cancer. 12(9):627–637.

Bruno G, Sparapano L. 2006. Effects of three esca–associated fungi on *Vitis vinifera* L.: I. Characterization of secondary metabolites in culture media and host responses to the pathogens in calli. Physiol Mol Plant Pathol. 69(4–6):209–223.

Bulley SM, Rassam M, Hoser D, Otto W, Schünemann N, Wright M, MacRae E, Gleave A, Laing W. 2009. Gene expression studies in kiwifruit and gene over–expression in *Arabidopsis* indicates that GDP–L–galactose guanyltransferase is a major control point of vitamin C biosynthesis. J Exp Bot. 60:765–778.

Cervilla LM, Blasco B, Ríos JJ, Romero L, Ruiz JM. 2007. Oxidative stress and antioxidants in tomato (*Solanum lycopersicum*) plants subjected to boron toxicity. Ann Bot. 100:747–756.

Chiapusio G, Sánchez AM, Reigosa MJ, González L, Pellissier F. 1997. Do germination indices adequately reflect allelochemical effects on the germination process?. J Chem Ecol. 23(11):2445–53.

Chong J, Xia J. 2020. Using Metaboanalyst 4.0 for metabolomics data analysis, interpretation, and integration with other omics data. In: Li S, editor. Computational methods and data analysis for metabolomics. Methods in molecular biology. New York: Humana; vol. 2104, p. 337–360.

Choudhury FK, Rivero RM, Blumwald E, Mittler R. 2017. Reactive oxygen species, abiotic stress and stress combination. Plant J. 90(5):856–867.

Chu M, Pedreño MA, Alburquerque N, Faize L, Burgos L, Almagro L. 2017. A new strategy to enhance the biosynthesis of *trans*–resveratrol by overexpressing stilbene synthase gene in elicited *Vitis vinifera* cell cultures. Plant Physiol Biochem. 113:141–148.

Clouse SD, Sasse JM. 1998. Brassinosteroids: essential regulators of plant growth and development. Annu Rev Plant Physiol Plant Mol Biol. 49:427–451.

D'Introno A, Paradiso A, Scoditti E, D'Amico L, De Paolis A, Carluccio MA, Nicoletti I, DeGara L, Santino A, Giovinazzo G. 2009. Antioxidant and anti–inflammatory properties of tomato fruits synthesizing different amounts of stilbenes. Plant Biotechnol J. 7(5):422–429.

Dai L, Zhou Q, Li R, Du Y, He J, Wang D, Cheng S, Zhang J, Wang Y. 2015. Establishment of a picloram–induced somatic embryogenesis system in *Vitis vinifera* cv. chardonnay and genetic transformation of a stilbene synthase gene from wild–growing *Vitis* species. Plant Cell Tissue Organ Cult. 121(2):397–412.

Delaunois B, Cordelier S, Conreux A, Cleḿent C, Jeandet P. 2009. Molecular engineering of resveratrol in plants. Plant Biotechnol J. 7:2−12.

Dewhirst RA, Fry SC. 2018. The oxidation of dehydroascorbic acid and 2,3–diketogulonate by distinct reactive oxygen species. Biochem J. 475(21):3451–3470.

Dietz K–J, Mittler R, Noctor G. 2016. Recent progress in understanding the role of reactive oxygen species in plant cell signaling. Plant Physiol. 171(3):1535–1539.

Dumont S, Rivoal J. 2019. Consequences of oxidative stress on plant glycolytic and respiratory metabolism. Front Plant Sci. 10:166.

Elshaer M, Chen Y, Xiu JW, Tang X. 2018. Resveratrol: an overview of its anti–cancer mechanisms. Life Sci. 207:340–349.

Elstner EF. 1987. Metabolism of activated oxygen species in the biochemistry of plants: a comprehensive treatise. In: Davies DD, editor. Amsterdam: Elsevier; vol. 8, p. 253–315.

Fariduddin Q, Khalil RRAE, Mir BA, Yusuf M, Ahmad A. 2013. 24–Epibrassinolide regulates photosynthesis, antioxidant enzyme activities and proline content of *Cucumis sativus* under salt and/or copper stress. Environ Monit Assess. 185(9):7845–7856.

Feng T, Chen SS, Gao DQ, Liu GQ, Bai HX, Li A, Peng LX. 2015. Selenium improves photosynthesis and protects photosystem II in pear (*Pyrus bretschneideri*), grape (*Vitis vinifera*), and peach (*Prunus persica*). Photosynthetica. 53(4):609–612.

Fisher AB. 2009. Redox signaling across cell membranes. Antioxid Redox Signal. 11:1349–1356.

Foyer CH, Shigeoka S. 2011. Understanding oxidative stress and antioxidant functions to enhance photosynthesis. Plant Physiol. 155(1):93–100.

Gertz M, Nguyen GTT, Fischer F, Suenkel B, Schlicker C, Fränzel B, Tomaschewski J, Aladini F, Becker C, Steegborn C. 2012. A molecular mechanism for direct sirtuin activation by resveratrol. PLoS ONE. 7(11):e49761.

Gill SS, Tuteja N. 2010. Reactive oxygen species and antioxidant machinery in abiotic stress tolerance in crop plants. Plant Physiol Biochem. 48:909–930.

Gónzalez–Urena A, Orea JM, Montero C, Jimenez JB. 2003. Improving post–harvest resistance in fruits by external application of trans–resveratrol. J Agric Food Chem. 51:82e89.

Grimmig B, Nuria Gonzalez–Perez M, Welzl G, Penuelas J, Schubert R, Hain R, Heidenreich B, Betz C, Langebartels C, Ernst D, Sandermann H. 2002. Ethylene– and ozone–induced regulation of a grapevine resveratrol synthase gene: different responsive promoter regions. Plant Physiol Biochem. 40(10):865–870.

Halliwell B, Gutteridge JMC. 1985. Free Radicals in Biology and Medicine. Oxford: Clarendon Press; p. 346.

Halls C, Yu O. 2008. Potential for metabolic engineering of resveratrol biosynthesis. Trends Biotechnol. 26(2):77–81.

Hammerschmidt R. 1999. Phytoalexins: what have we learned after 60 years?. Annu Rev Phytopathol. 37:285–306.

Harikumar KB, Aggarwal BB. 2008. Resveratrol: a multitargeted agent for age–associated chronic diseases. Cell Cycle. 7(8):1020–1035.

Hasan M, Bae H. 2017. An overview of stress–induced resveratrol synthesis in grapes: perspectives for resveratrol–enriched grape products. Molecules. 14;22(2):294.

Huang S, Van Aken O, Schwarzländer M, Belt K, Millar AH. 2016. The roles of mitochondrial reactive oxygen species in cellular signaling and stress responses in plants. Plant Physiol. 171:1551–1559.

Hussein HAA, Mekki BB, Abd El-Sadek ME, El Lateef EE. 2019. Effect of L-Ornithine application on improving drought tolerance in sugar beet plants. Heliyon 5(10): e02631.

Jain AK, Nessler CL. 2000. Metabolic engineering of an alternative pathway for ascorbic acid biosynthesis in plants. Molecular Breeding. 6:73–78.

Janeczko A, Skoczowski A. 2005. Mammalian sex hormones in plants. Folia Histochem Cytobiol. 43(2):71–79.

Jia M, Li D, Colombo R, Wang Y, Wang X, Cheng T, Zhu Y, Yao X, Xu C, Ouer G, Li H, Zhang C. 2019. Quantifying chlorophyll fluorescence parameters from hyperspectral reflectance at the leaf scale under various nitrogen treatment regimes in winter wheat. Remote Sensing. 11(23):2838.

Juan CA, Pérez de la Lastra JM, Plou FJ, Pérez–Lebeña E. 2021. The chemistry of reactive oxygen species (ROS) revisited: outlining their role in biological macromolecules (DNA, lipids and proteins) and induced pathologies. Int J Mol Sci. 22(9):4642.

Kanduja KL, Hardwaj A, Kaushik G. 2004. Resveratrol inhibits N-nitrosodiethylamine-induced ornithine decarboxylase and cyclooxygenase in mice. J. Nutr. Sci. Vitamin. 50(1): 61-65.

Kerepesi I, Galiba G. 2000. Osmotic and salt stress–induced alteration in soluble carbohydrate content in wheat seedlings. Crop Sci. 40(2):482.

King RE, Bomser JA, Min DB. 2006. Bioactivity of resveratrol. Compr Re Food Sci Food Saf. 5(3):65–70.

Kopka J, Schauer N, Krueger S, Birkemeyer C, Usadel B, Bergmüller E, Dörmann P, Weckwerth W, Gibon Y, Stitt M. 2005. GMD@CSB.DB: the golm metabolome database. Bioinformatics. 21:1635–1638.

Kostopoulou Z, Therios I, Molassiotis A. 2014. Resveratrol and its combination with α–tocopherol mediate salt adaptation in citrus seedlings. Plant Physiol Biochem. 78:1–9.

Koyro H–W, Ahmed P, Geissler N. 2012. Abiotic stress response in plants: an overview. In: Ahmed P, Prasad MNV, editors. Environmental adaptation and stress tolerance of plants in the era of climate change. Dordrecht: Springer; 515p.

Laing WA, Martínez–Sánchez M, Wright MA, Bulley SM, Brewster D, Dare AP, Rassam M, Wang D, Storey R, Macknight RC, Hellens RP. 2015. An upstream open reading frame is essential for feedback regulation of ascorbate biosynthesis in *Arabidopsis*. Plant Cell. 27(3):772–786.

Laing WA, Wright MA, Cooney J, Bulley SM. 2007. The missing step of the L–galactose pathway of ascorbate biosynthesis in plants, an L–galactose guanyltransferase, increases leaf ascorbate content. PNAS. 104:9534–9539.

Landi M, Misra BB, Muto A, Bruno L, Araniti F. 2020. Phytotoxicity, morphological, and metabolic effects of the sesquiterpenoid nerolidol on *Arabidopsis thaliana* seedling roots. Plants. 9:1347.

Levandoski NG, Baker EM, Canham JE. 1964. A monodehydro form of ascorbic acid in the autoxidation of ascorbic acid to dehydroascorbic acid. Biochemistry. 3(10):1465–1469.

Li J, Yang Y, Sun K, Chen Y, Chen X, Li X. 2019. Exogenous melatonin enhances cold, salt and drought stress tolerance by improving antioxidant defense in tea plant (*Camellia sinensis* (L.) O. Kuntze). Molecules. 24(9):1826.

Lisec J, Schauer N, Kopka J, Willmitzer L, Fernie AR. 2006. Gas chromatography mass spectrometry–based metabolite profiling in plants. Nat Protoc. 1(1):387–396.

Liu J–H, Wang W, Wu H, Gong X, Moriguchi T. 2015. Polyamines function in stress tolerance: from synthesis to regulation. Front Plant Sci. 6:827.

Liu MQ, Ma FL, Jiang CY, Wang YJ. 2019. Expression of stilbene synthase VqSTS6 from wild Chinese *Vitis quinquangularis* in grapevine enhances resveratrol production and powdery mildew resistance. Planta. 250:1997–2007.

Liu R–X, Zhou ZG, Guo WQ, Chen B–L, Oosterhuis DM. 2008. Effects of N fertilization on root development and activity of water–stressed cotton (*Gossypium hirsutum* L.) plants. Agric Water Manag. 95(11):1261–1270.

Livingston DP, Hincha DK, Heyer AG. 2009. Fructan and its relationship to abiotic stress tolerance in plants. Cell Mol Life Sci. 66:2007–2023.

Lorence A, Chevone BI, Mendes P, Nessler CL. 2004. *myo*–Inositol oxygenase offers a possible entry point into plant ascorbate biosynthesis. Plant Physiol. 134(3):1200–1205.

Malone SR, Mayeux HS, Johnson HB, Polley HW. 1993. Stomatal density and aperture length in four plant species grown across a subambient CO_2 gradient. Am J Bot. 80(12):1413–1418.

Mantovanelli GC, Mito MS, Moreira da Costa Menezes PV, Contesoto IdeC, Alves do Nascimento CR, Wagner Zampieri AL, Stulp GF, Constantin RP, Ishii–Iwamoto EL. 2020. Differential effects of exogenous resveratrol on the growth and energy metabolism of *Zea mays* and the weed *Ipomoea grandifolia*. J Agric Food Chem. 68:3006–3016.

Martin–Tanguy J. 2001. Metabolism and function of polyamines in plants: recent development (new approaches). Plant Growth Regul. 34(1)135–148.

Martínez-Peñalver A, Pedrol N, Reigosa MJ, Sánchez-Moreiras AM. 2012. Tolerance of *Arabidopsis thaliana* to the allelochemical protocatechualdehyde. J. Plant Growth Regul. 31(3): 406-415.

Mattio LM, Catinella G, Dallavalle S, Pinto A. 2020. Stilbenoids: a natural arsenal against bacterial pathogens. Antibiotics. 9:336.

Maxwell K, Johnson GN. 2000. Chlorophyll fluorescence—a practical guide. J Exp Bot. 51:659–668.

Mittler R, Blumwald E. 2010. Genetic engineering for modern agriculture: challenges and perspectives. Annu Rev Plant Biol. 61(1):443–462.

Mittler R, Vanderauwera S, Gollery M, Van Breusegem F. 2004. Reactive oxygen gene network of plants. Trends Plant Sci. 9:490–498.

Mohapatra S, Minocha R, Long S, Minocha SC. 2009. Putrescine overproduction negatively impacts the oxidative state of poplar cells in culture. Plant Phys. Biochem. 47(4): 262-271

Murakeözy ÉP, Nagy Z, Duhazé C, Bouchereau A, Tuba Z. 2003. Seasonal changes in the levels of compatible osmolytes in three halophytic species of inland saline vegetation in Hungary. J Plant Physiol. 160(4):395–401.

Pociecha E, Janeczko Z, Janeczko A. 2014. Resveratrol stimulates phenolic metabolism and PSII efficiency in wheat infected with powdery mildew. J Plant Interact. 9(1):494−503.

Prieto P, Peñuelas J, Llusià J, Asensio D, Estiarte M. 2009. Effects of long–term experimental night–time warming and drought on photosynthesis, *F*v/*F*m and stomatal conductance in the dominant species of a Mediterranean shrubland. Acta Physiol Plant. 31(4):729–739.

Rai VK. 2002. Role of amino acids in plant responses to stresses. Biol Plant. 45(4):481–487.

Salehi B, Mishra A, Nigam M, Sener B, Kilic M, Sharifi–Rad M, Fokou P, Martins N, Sharifi–Rad J. 2018. Resveratrol: a double–edged sword in health benefits. Biomedicines. 6:91.

Sarafi E, Tsouvaltzis P, Chatzissavvidis C, Siomos A, Therios I. 2017. Melatonin and resveratrol reverse the toxic effect of high boron (B) and modulate biochemical parameters in pepper plants (*Capsicum annuum* L.). Plant Physiol Biochem. 112:173–182.

Sharma P, Jha AB, Dubey RS, Pessarakli M. 2012. Reactive oxygen species, oxidative damage, and antioxidative defense mechanism in plants under stressful conditions. J Botany. 1–26.

Shi J, He M, Cao J, Wang H, Ding J, Jiao Y, Li R, He J, Wang D, Wang Y. 2014. The comparative analysis of the potential relationship between resveratrol and stilbene synthase gene family in the development stages of grapes (*Vitis quinquangularis* and *Vitis vinifera*). Plant Physiol Biochem. 74:24–32.

Shishodia S, Aggarwal BB. 2006. Resveratrol in health and disease. In: Aggarwal BB, Shishodia S, editors. Resveratrol: a polyphenol for all seasons. New York: CRC Press; p. 1–16.

Smirnoff N, Wheeler GL. 2000. Ascorbic acid in plants: biosynthesis and function. Crit Rev Plant Sci. 19(4):267–290.

Stojanović S, Sprinz H, Brede O. 2001. Efficiency and mechanism of the antioxidant action of trans–resveratrol and its analogues in the radical liposome oxidation. Arch Biochem Biophys. 391(1):79–89.

Sumner LW, Amberg A, Barrett D, Beale MH, Beger R, Daykin CA, Fan TWM, Fiehn O, Goodacre R, Griffin JL. 2007. Proposed minimum reporting standards for chemical analysis. Metabolomics. 3:211–221.

Tanaka S, Aoshima K. 2010. MassBank: A public repository for sharing mass spectral data for life sciences. J Mass Spectrom. 45:703–714.

Tang K, Zhan J–C, Yang H–R, Huang W–D. 2010. Changes of resveratrol and antioxidant enzymes during UV–induced plant defense response in peanut seedlings. J Plant Physiol. 167(2):95–102.

Truong V–L, Jun M, Jeong W–S. 2018. Role of resveratrol in regulation of cellular defense systems against oxidative stress. BioFactors. 44(1):36–49.

Tsugawa H, Cajka T, Kind T, Ma Y, Higgins B, Ikeda K, Kanazawa M, VanderGheynst J, Fiehn O, Arita M. 2015. MS–DIAL: data–independent MS/MS deconvolution for comprehensive metabolome analysis. Nat Meth. 12:523.

Van den Ende W, Valluru R. 2009. Sucrose, sucrosyl oligosaccharides, and oxidative stress: scavenging and salvaging?. J Exp Bot. 60:9–18.

Vestergaard M, Ingmer H. 2019. Antibacterial and antifungal properties of resveratrol. Int J Antimicrob Agents. 53:716–723.

Wolter F, Turchanowa L, Stein J. 2003. Resveratrol-induced modification of polyamine metabolism is accompanied by induction of c-Fos. Carcinogen. 24(3): 469-474.

Xu Z, Zhou G. 2008. Responses of leaf stomatal density to water status and its relationship with photosynthesis in a grass. J Exp Bot. 59(12):3317–3325.

Zhang G–Y, Liu R–R, Zhang C–Q, Tang K–X, Sun M–F, Yan G–H, Liu Q–Q. 2015. Manipulation of the rice L–galactose pathway: evaluation of the effects of transgene overexpression on ascorbate accumulation and abiotic stress tolerance. PLoS ONE. 10(5):e0125870.

Zheng S, Zhao S, Li Z, Wang Q, Yao F, Yang L, Pan L, Liu W. 2015. Evaluating the effect of expressing a peanut resveratrol synthase gene in rice. PLoS ONE. 10(8):e0136013.

Figure 1. Dose–response curves of initial growth of *L. sativa* seedlings exposed to increasing doses of resveratrol (6.25–400 µM). (A) germination, (B) root length, (C) root fresh weight, (D) aerial part fresh weight, (E) root dry weight, and (F) aerial part dry weight. ED_{50}: dose causing 50% stimulus of aerial part fresh weight compared to the control. Significant differences between means were identified by ANOVA with Tukey's test ($p \leq 0.05$). * ($p \leq 0.05$), ** ($p \leq 0.01$), *** ($p \leq 0.001$). $n = 3$.

Figure 2. Semi–quantitative determination of H_2O_2 in *L. sativa* leaves treated with resveratrol 100 µM, showing the localization of the hydrogen peroxide on leaf surface after DAB staining: (A) control leaf and (B) treated leaf. Image magnification 4X, scale bar 200 µm.

Figure 3. *In situ* $O_2^{\cdot -}$ localization in resveratrol 100 µM treated and non–treated *L. sativa* leaves, showing the localization of the superoxide on leaf surface after NBT staining: (A) control leaf and (B) treated leaf. Image magnification 4X, scale bar 200 µm.

Figure 4. Micrograph of the stomatal density of non–treated (A) and resveratrol–treated (B) leaves of *L. sativa*. Stomatal density (C), width (D), and length (E) of treated and non–treated leaves with 100 µM resveratrol. Asterisks indicate significant differences between mean values (n = 6) of treated and control plants after *t*-test ($p \leq 0.05$). * ($p \leq 0.05$), ** ($p \leq 0.01$), *** ($p \leq 0.001$). Magnification 20X, scale bar 20 µm.

Figure 5. Effects of resveratrol 100 µM on the leaf osmotic potential [$\Psi(\pi)$] of *L. sativa*. Significant differences between means were identified by *t*-test ($p \leq 0.05$). n = 5.

Figure 6. The maximum quantum efficiency of dark-adapted PSII (Fv/Fm) (A), the apparent electron transport rate (ETR) (B), the effective PSII photochemical quantum yield (C) (ϕ_{II}), the quantum yield of regulated emission of energy in the form of heat (ϕ_{NPQ}) (D), and the non–regulated emission of energy in the form of fluorescence (ϕ_{NO}) (E) in non–treated and treated (100 µM resveratrol) lettuce seedlings. Significant differences between means were identified by *t*-test with ($p \leq 0.05$). * ($p \leq 0.05$), ** ($p \leq 0.01$), *** ($p \leq 0.001$). AU = Arbitrary Units. n = 4.

Figure 7. (A) Pathway enrichment analysis revealed different metabolic pathways enriched during resveratrol treatment (p-value cut off ≤ 0.05). (B) Results from "Pathway Analysis" carried on the concentrations of metabolite identified in resveratrol–treated and non–treated seedlings. Total Cmpd: the total number of compounds in the pathway; Hits: the matched number from the uploaded data; Raw p is the original p-value; –Log(p) value: the logarithm of the original p–value calculated from the enrichment analysis; Holm adjust: the Holm adjustment used to counteract the problem of multiple comparisons; FDR: the false discovery rate applied to the nominal p–values to control for false–positive findings; Impact: the pathway impact value calculated from the combination of enrichment and topology analysis.

Figure 8. (A) Principal component analysis (PCA) and (B) partial least square discriminant analysis (PLS–DA) showing score plots discriminating the C (control) and T (resveratrol–treated) groups by virtue of the first 2 PCs. (C) PLS–DA derived analysis variable importance of projection (VIP) features for the groups and (D) overlay heat map of the significantly affected metabolites (selected by t–test with $p \leq 0.05$). Each square represents the different stage's effect on every metabolite's relative abundance using a false–color scale. Dark-red, and blue indicate relative metabolite abundances, increased and decreased, respectively. n = 6.

Table 1. Metabolites differentially accumulated in the control and resveratrol–treated samples. Data were analyzed through Student's *t*–test ($p \leq 0.05$). A False Discovery Rate (FDR) was applied to the nominal *p*–values to control for false–positive findings. Negative values of the *t*–stat indicate a significant increase of the specific metabolite in resveratrol–treated seedlings. ($n = 6$).

Metabolites	*t*–stat	*p*–value	FDR	Class
Hexacosane	–2.9796	0.013818	0.024022	Alkane
DL–Allothreonine	–6.77	4.92E–05	0.00015	
DL–Pyroglutamic acid	–2.9538	0.014442	0.024357	
Glycine	–3.866	0.003129	0.005994	
Lysine	–7.1036	3.28E–05	0.000103	
L–Alanine	–9.9057	1.73E–06	7.84E–06	
L–Aspartic acid	–7.1904	2.96E–05	9.84E–05	Amino acid
L–Glutamic acid	–10.114	1.43E–06	7.55E–06	
L–Isoleucine	–6.3214	8.67E–05	0.000239	
L–Norleucine	–6.5114	6.80E–05	0.000197	
L–Norvaline	–4.2893	0.001588	0.003204	
L–Serine	–5.6616	0.000209	0.00049	
L–Valine	–4.2538	0.001679	0.003329	
Galactosamine	–4.2064	0.00181	0.003527	Amino sugar
Cafferic acid	–2.9263	0.015137	0.025154	
Creatinine	61.681	0.000106	0.000272	
DL–ß–Hydroxybutyric acid	25.241	2.18E–10	4.11E–09	
Glucose 6–phosphate	–10.682	8.66E–07	5.43E–06	
Glycerol–3–galactoside	73.477	2.46E–05	8.42E–05	
Dehydroascorbic acid	–6.2487	9.52E–05	0.000253	
Methylamine	–5.5625	0.00024	0.000534	
N–Acetylornithine	–2.9698	0.01405	0.024055	
N–Acetyl–D–glucosamine	–27.628	8.95E–11	2.18E–09	Miscellaneous
Phosphate	–37.609	4.21E–12	4.76E–10	
Uridine 5'–diphospho–*N*–acetylglucosamine	–15.304	2.88E–08	2.96E–07	
Xylonolactone	–5.1024	0.000462	0.000986	
1,6–Anhydro–ß–D–glucose	–5.6503	0.000212	0.00049	
3–Amino isobutyric acid	–2.7135	0.021801	0.035703	
2,3–Dihydroxybenzoate	–7.8281	1.42E–05	5.03E–05	
4–Hydroxyphenylacetic acid	–9.1653	3.51E–06	1.42E–05	
5–Keto–D–gluconate	–6.518	6.74E–05	0.000197	
Glutaric acid	–6.2388	9.65E–05	0.000253	
Glyceric acid	84.732	7.09E–06	2.67E–05	
Methylmalonic acid	3.474	0.005981	0.010728	Organic acid
Oxalic acid	–3.7346	0.003881	0.007309	
Oxamic acid	–4.3671	0.001406	0.002888	
Succinic acid	99.904	1.60E–06	7.55E–06	

Tartrate	–5.821	0.000168	0.000413	
Threonic acid	57.757	0.000179	0.00043	
Uridine	58.723	0.000157	0.000394	Pyrimidine
L–Ornithine	–10.033	1.54E–06	7.55E–06	Polyamine
Putrescine	27.422	9.63E–11	2.18E–09	
Arabinose	–7.1229	3.21E–05	0.000103	
Cellobiose	–7.9975	1.18E–05	4.30E–05	
Fructose	–3.0832	0.011578	0.020442	
Galactose	–30.953	2.91E–11	1.64E–09	
Gentiobiose	–12.547	1.92E–07	1.45E–06	
Isomaltose	–5.5594	0.000241	0.000534	
Lactose	–10.017	1.57E–06	7.55E–06	
Lactulose	–9.3589	2.91E–06	1.23E–05	Sugar
L–Arabinose	–29.163	5.24E–11	1.97E–09	
L–Rhamnose	10.146	1.39E–06	7.55E–06	
Mannose	35.198	0.00554	0.010098	
Melibiose	–12.685	1.73E–07	1.40E–06	
Sophorose	–16.15	1.72E–08	2.15E–07	
Trehalose	–8.8309	4.91E–06	1.91E–05	
Xylose	–13.096	1.28E–07	1.20E–06	
Lactobionic acid	–12.07	2.77E–07	1.84E–06	Sugar acid
Glucosaminic acid	–24.524	2.90E–10	4.68E–09	
Galactinol	–10.123	1.42E–06	7.55E–06	
Glycerol	–3.5777	0.005031	0.009319	
Inositol	–16.876	1.12E–08	1.58E–07	
Lactitol	–15.483	2.58E–08	2.91E–07	
L–Iditol	–9.346	2.94E–06	1.23E–05	Sugar alcohol
Maltitol	–12.149	2.60E–07	1.84E–06	
meso–Erythritol	–4.3951	0.001345	0.002815	
Palatinitol	–12.85	1.53E–07	1.33E–06	
Xylitol	–5.4559	0.000279	0.000605	

Figure 1

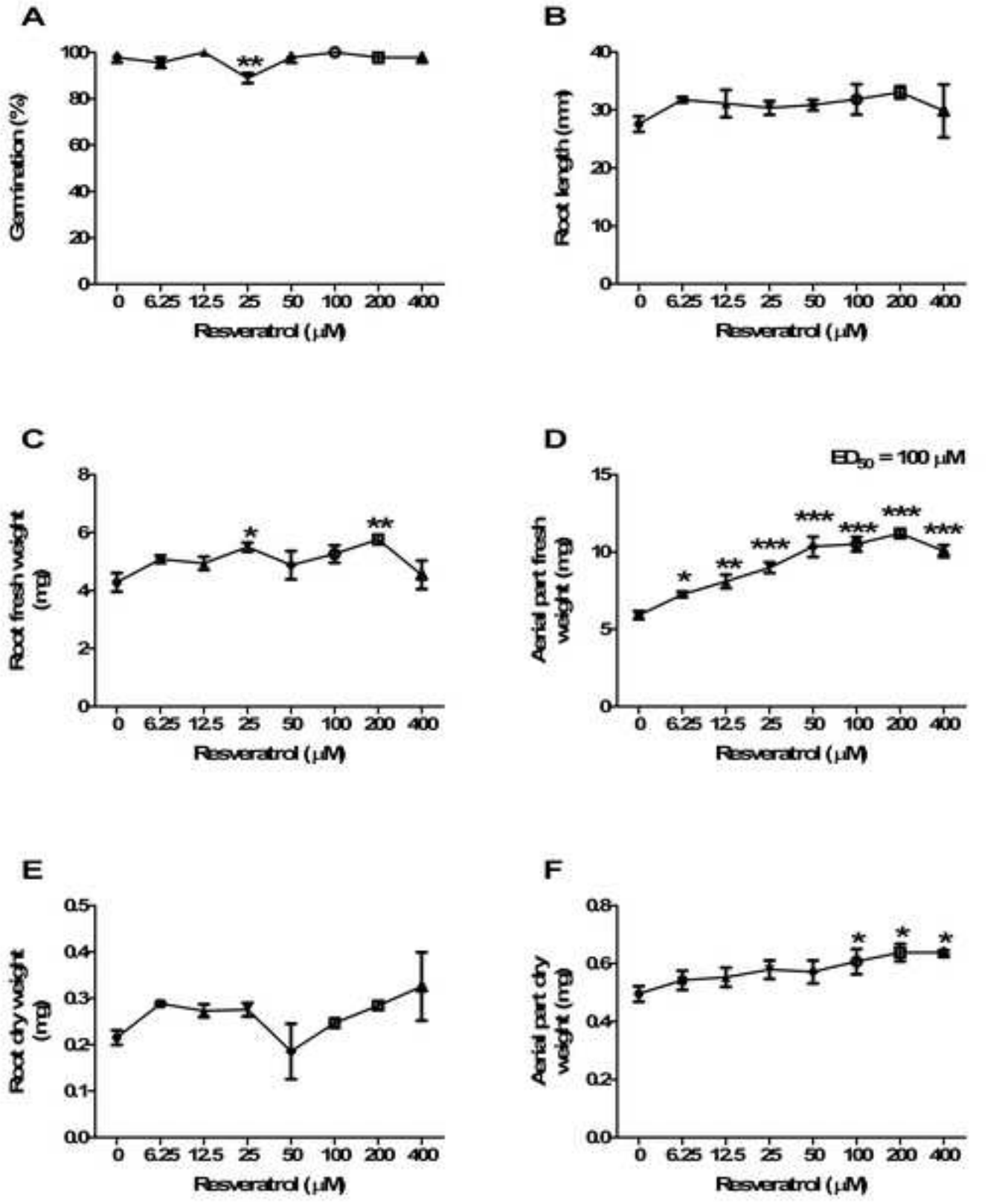

Figure 2

Click here to access/download;Figure;Fig.2.tif

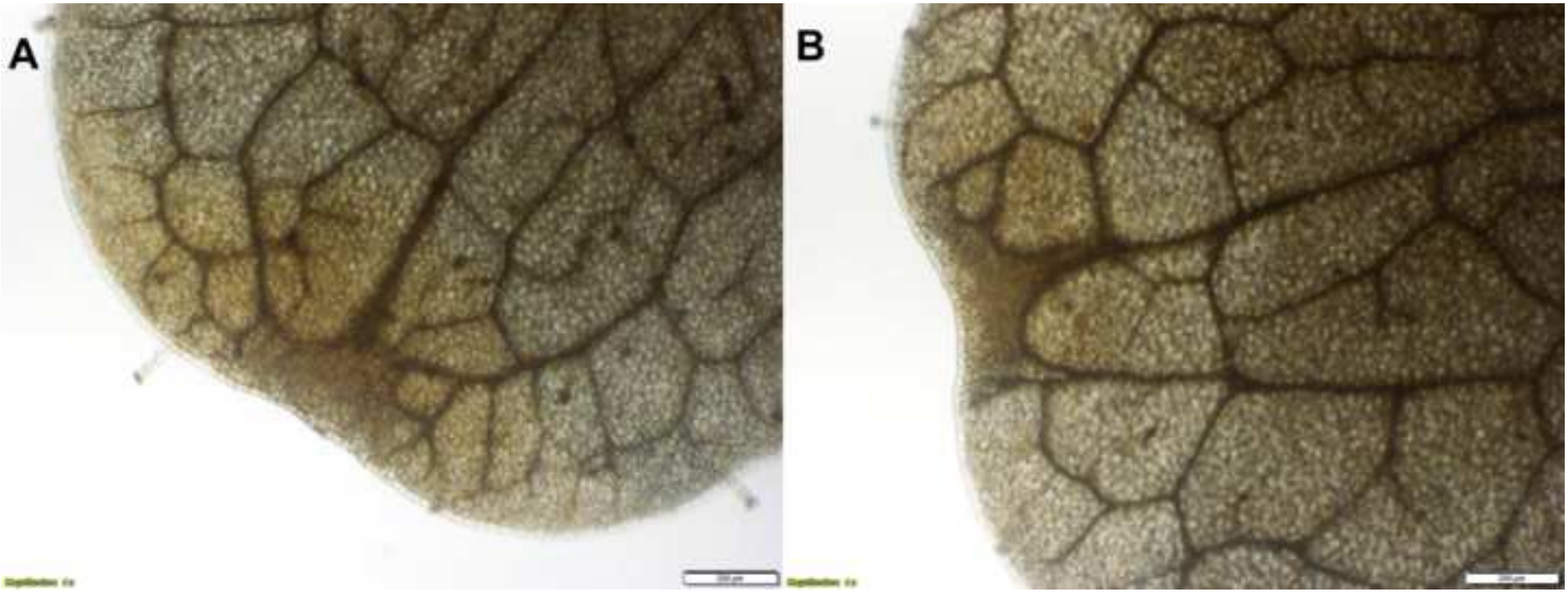

Figure 3

Click here to access/download;Figure;Fig.3.tif

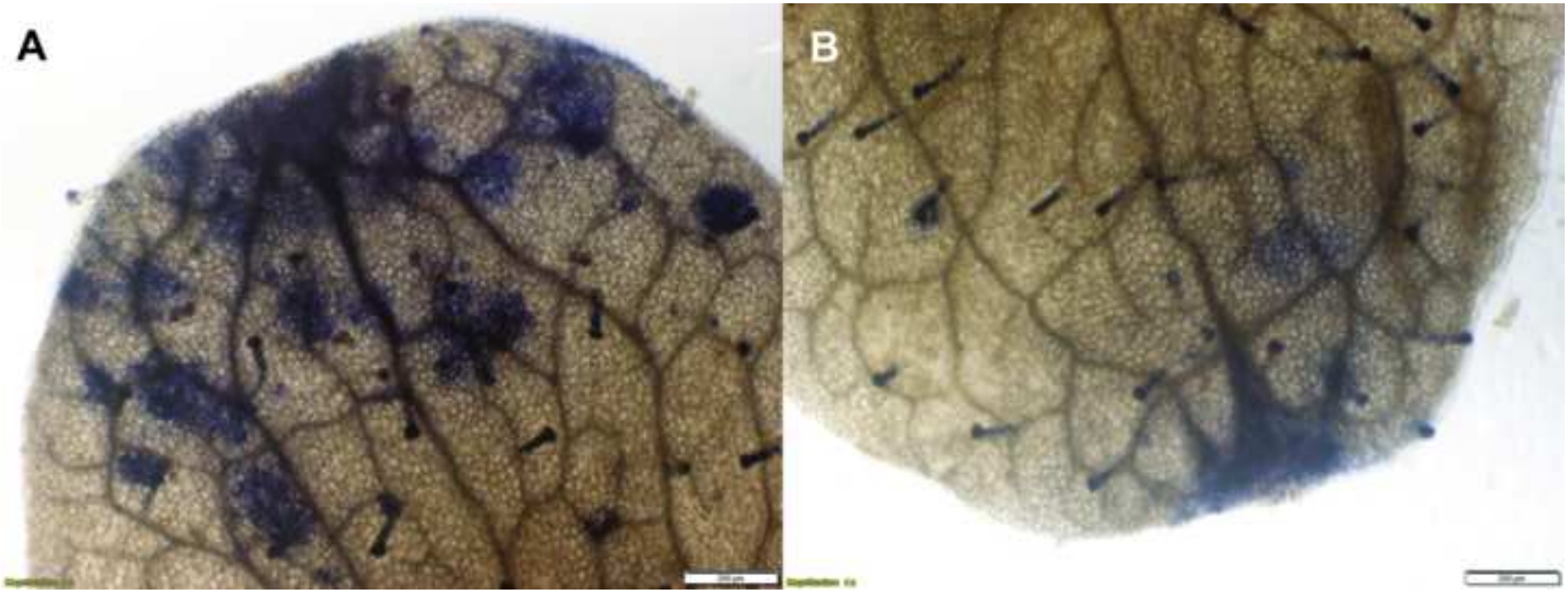

Figure 4

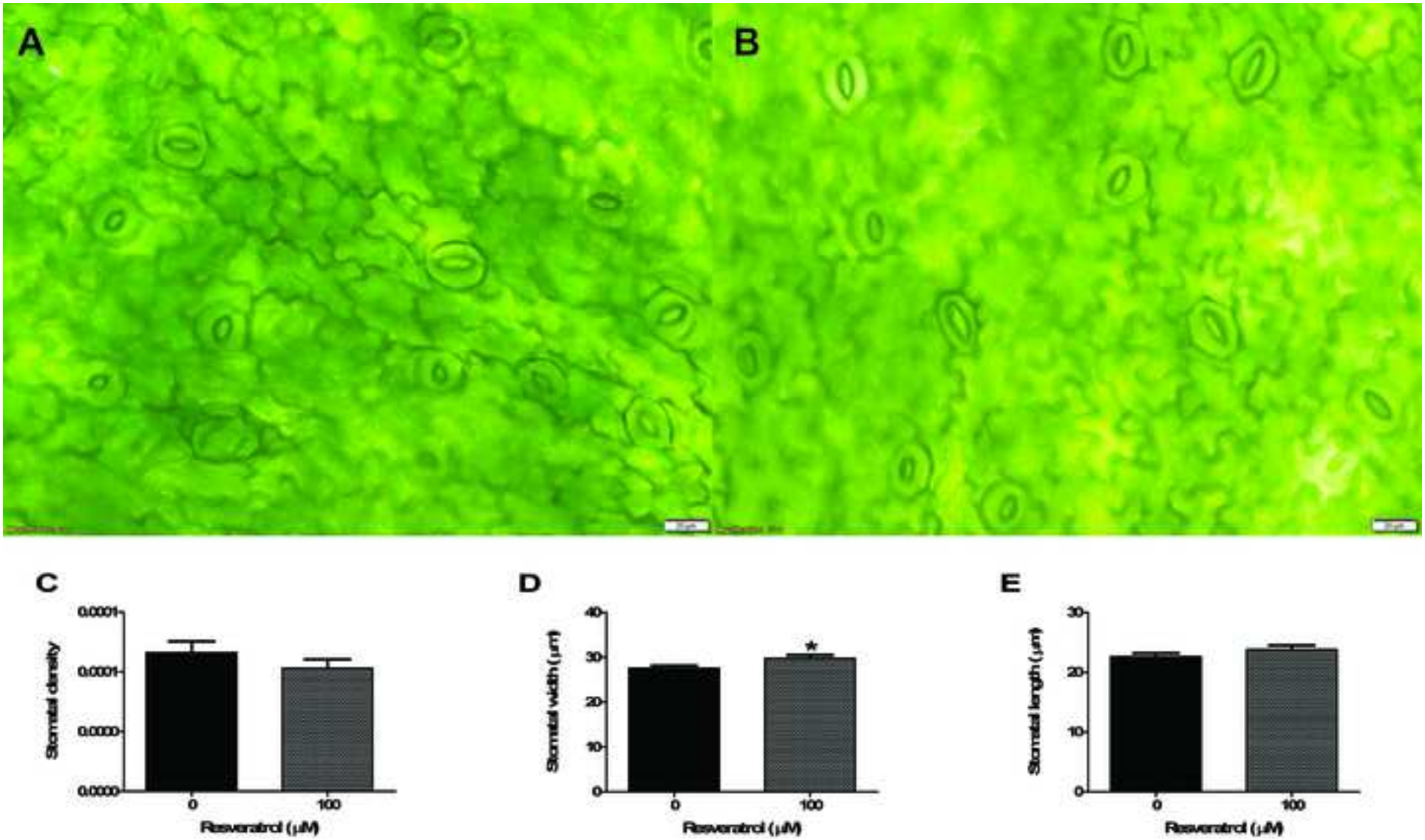

Figure 5

Click here to access/download;Figure;Fig.5.tif

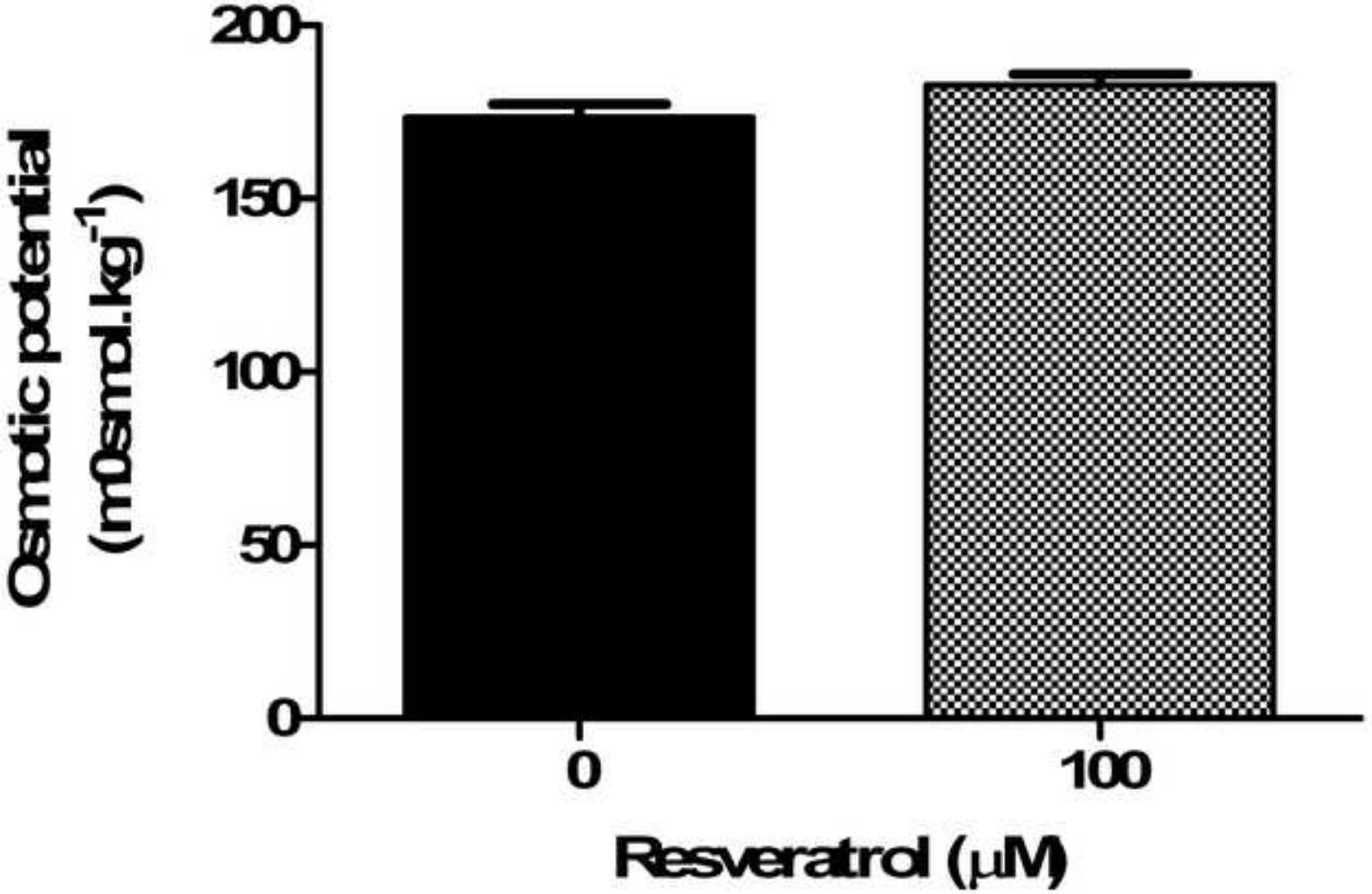

Figure 6

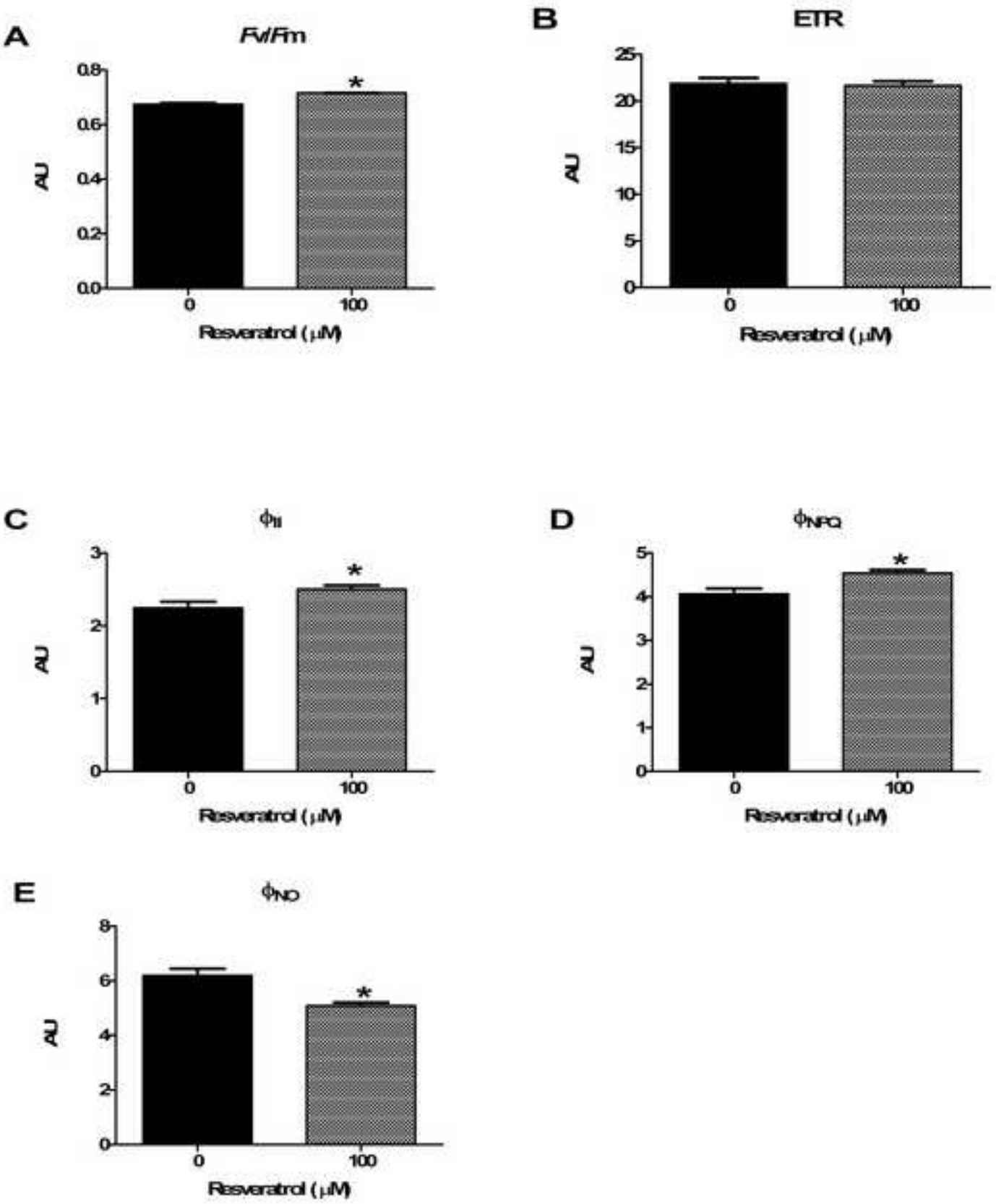

Figure 7

Click here to access/download;Figure;Fig.7.tif

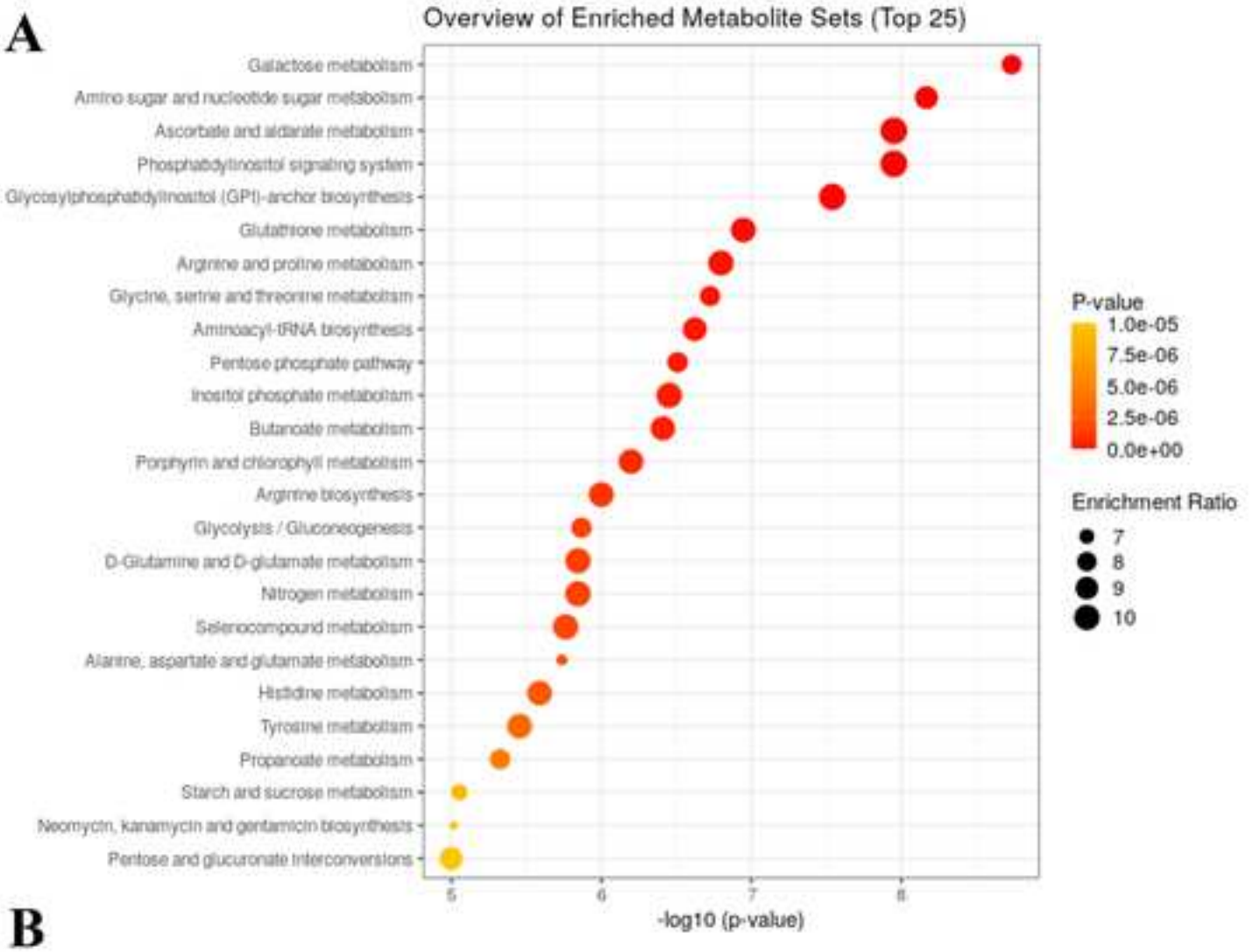

B

	Total Cmpd	Hits	Raw p	-LOG10(p)	Holm adjust	FDR	Impact
Starch and sucrose metabolism	22	5	3.06E-05	4.5149	0.00068073	5.41E-05	0.63853
Alanine aspartate and glutamate metabolism	22	5	2.89E-07	6.5384	1.19E-05	2.22E-06	0.57914
Glycine serine and threonine metabolism	33	5	1.67E-06	5.7761	4.86E-05	4.20E-06	0.41558
Arginine biosynthesis	18	4	1.00E-06	5.9992	3.41E-05	3.54E-06	0.36117
Galactose metabolism	27	8	1.58E-07	6.801	6.80E-06	1.82E-06	0.25476
beta-Alanine metabolism	18	3	6.31E-05	4.2003	0.001072	9.67E-05	0.25397
Glyoxylate and dicarboxylate metabolism	29	7	1.51E-05	4.8217	0.00037688	3.15E-05	0.22451
Pantothenate and CoA biosynthesis	23	3	0.015483	1.8101	0.092898	0.017371	0.21166

Figure 8

Click here to access/download;Figure;Fig.8.tif